Chinese Chemical Letters 37 (2026) 112355

Contents lists available at ScienceDirect

Chinese Chemical Letters

journal homepage: www.elsevier.com/locate/cclet

Macrocycle-confined dimeric cobalt-porphyrin for boosted transport of anions

Fei Zeng[a,b], Xinrui Pan[a], Zihong Yang[a], Jie Shen[a], Wenju Chang[a,*], Huaqiang Zeng[a,*]

[a] Fujian Provincial Key Laboratory of Molecular Synthesis and Functional Discovery and College of Chemistry, Fuzhou University, Fuzhou 350108, China
[b] College of Pharmacy, Xiangnan University, Chenzhou 423099, China

ARTICLE INFO

Article history:
Received 14 October 2025
Revised 23 December 2025
Accepted 30 December 2025
Available online 30 December 2025

Keywords:
Supramolecular chemistry
Ion transport
Giant macrocycle
Adaptive cavity
Confined metalloporphyrin

ABSTRACT

We demonstrate here a macrocyclic host capable of simultaneously binding two Co^{2+}-porphyrin complexes in its adaptive giant cavity. Such a geometrically confined porphyrin dimer promotes highly efficient transport of anions across the lipid membrane by virtue of dynamic metal-anion bonding interactions, which is in sharp contrast to the most studied class of anionphores that mediates anion transport through intermolecular H-bonds. The transport activity increases in the order of Br^-, Cl^-, ClO_4^- and NO_3^-, with the corresponding EC_{50} values of 0.57, 0.69, 0.74 and 1.30 μmol/L, and transport rate enhancements by up to ~35 folds over the monomeric Co^{2+}-porphyrin complex. The determined binding constants suggest **1**-mediated cooperative binding toward **G3** molecules might account for the unique behavior by Co^{2+} with respect to other metal ions.

© 2026 Published by Elsevier B.V. on behalf of Chinese Chemical Society and Institute of Materia Medica, Chinese Academy of Medical Sciences.

Maintaining transmembrane electrochemical gradients *via* tightly controlled ion homeostasis is crucial for regulating cellular activities, a process that largely depends on channel proteins [1,2]. Through regulating the movement of Cl^- anions, multiple chloride channels help to determine cell membrane potential, modify cell cycle, adhesion and cell motility, maintain intracellular pH and cell volume, *etc.* Malfunctioning chloride channels may result in respiratory, neuromuscular and renal dysfunction and diseases such as cystic fibrosis. This has inspired the search for artificial transmembrane anion transporters to emulate functions of natural systems, shed light into transport mechanisms or serve as possible therapeutics [3–20].

Although investigation of transmembrane anion transporter has intensified in recent years, anion transport has been predominantly mediated by diverse anionophores capable of H-bonding to anions [3–16,21–37]. Yet, a great variety of innovative strategies that do not rely on intermolecular H-bonds for facilitated cross-membrane anion transport have also emerged, creatively applying halogen bonds [38–41], chalcogen bonds [42–44], pnictogen bonds [45,46], anion–π interactions [47–49], charge repulsion [50], bidentate phosphonium boranes [51] and cage structures [52,53] as well as side chain-side chain interactions [54–56] or intramolecular folding of aromatic foldamers [57] that create hollow sizable cavities.

Another inspiring strategy takes advantage of limitedly studied dynamic metal-anion interactions of metalloporphyrins to induce anion transport across the membrane [58-61]. Metalloporphyrins feature four pyrroline subunits interconnected *via* methane bridges in a circular fashion, with a metal ion sitting in the ring center that leaves up to two labile axial coordination sites available for anion binding. As early as 1996, Cuppoletti *et al.* reported increased anion permeability in lung epithelial cells caused by a Mn(III)-bound metalloporphyrin chloride. Mao and his co-workers extended the study further, establishing that this metalloporphyrin induced autophagy and immunogenic cell death [59]. Structure-wise, these anion transporters are based on monomeric [58,59] organometallic complexes. Here, we describe another alternative approach, employing a dimeric Co^{2+}-porphyrin confined within an adaptive macrocyclic tubular cavity to achieve very substantial enhancements in anion transport activity by up to 35 folds over the monomeric Co^{2+}-porphyrin complex.

Recently we reported a naphthalene diimide-based giant macrocycle **1**, possessing a giant hexagon-shaped tubular cavity of up to 15.3 and 14.6 Å when fully stretched (Fig. 1a) [60]. This giant cavity demonstrates an adaptive feature in response to the guest molecule pagoda[5]arene [61], exhibiting a smaller cavity in the guest's absence that becomes much larger in its presence (Fig. 1b). Inspired by these early results, we hypothesized that the adaptive

* Corresponding authors.
E-mail addresses: wenjuchang@fzu.edu.cn (W. Chang), hqzeng@fzu.edu.cn (H. Zeng).

https://doi.org/10.1016/j.cclet.2025.112355
1001-8417/© 2026 Published by Elsevier B.V. on behalf of Chinese Chemical Society and Institute of Materia Medica, Chinese Academy of Medical Sciences.

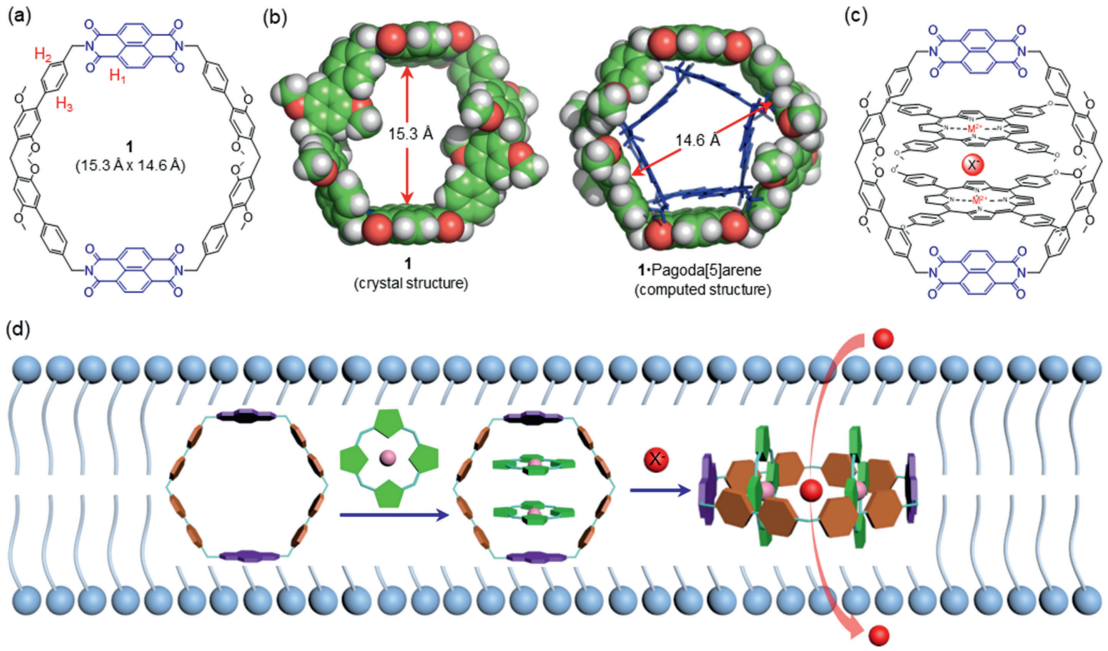


Fig. 1. (a) Structure of host **1**. (b) Crystal and computed structures of **1** and complex **1**·pagoda[5]arene [60], illustrating an adaptive nature of the interior cavity. (c) A possibly formed 1:2 sandwich supramolecular structure of **1** with an anion-bound dimeric metalloporphyrin. (d) Proposed self-assembly process for forming a supramolecular ensemble for facilitating transmembrane anion transport.

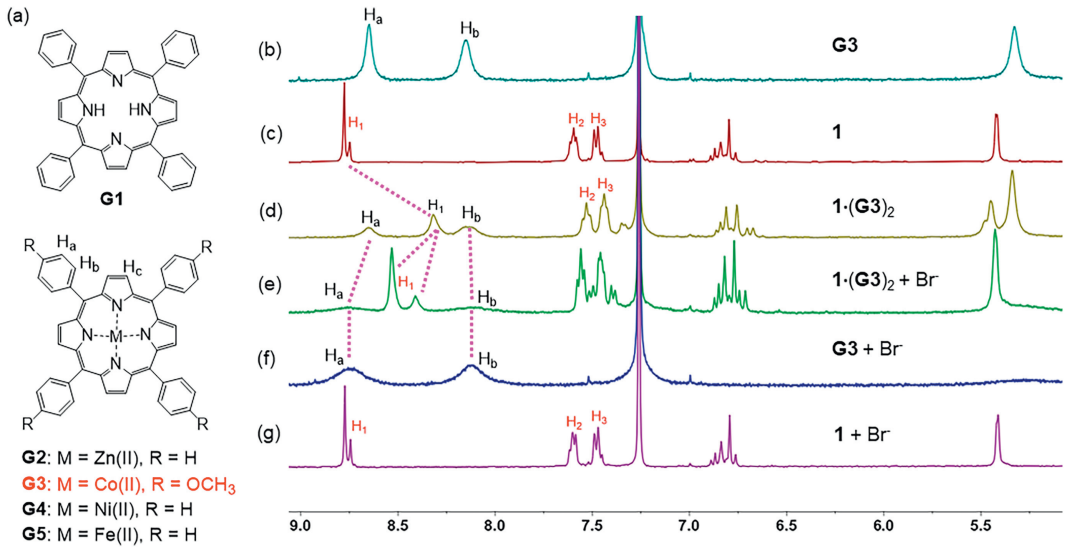


Fig. 2. Structures of **Gn**s (a) and partial ^{1}H NMR spectra (400 MHz, $CDCl_3$, 298 K) of (b) **G3**, (c) **1**, (d)**1**·(**G3**)$_2$, (e) **1**·(**G3**)$_2$ + 10 equiv. of Br^-, (f) **G3** + 10 equiv. of Br^- and (g) **1** + 10 equiv. of Br^-. [**1**] = [**1**·(**G3**)$_2$] = 1.0 mmol/L and [**G3**] = 2.0 mmol/L.

giant cavity in **1** might be capable of binding electron-rich porphyrins (**G1**) or metalloporphyrins (**Gn**s, $n = 2$-5).

Indeed, through our current continued investigation of **1**-mediated host-guest chemistry, we demonstrate here that **1** can bind two **Gn** molecules in its giant cavity, forming a sandwiched 1:2 host-guest complex **1**·(**Gn**)$_2$ (Fig. 1c). And to our best knowledge, this is the first example of cavity-containing hosts that can bind two porphyrin molecules in its adaptive cavity. Further, we show that such a dimeric Co^{2+}-porphyrin (**G3**)$_2$ geometrically confined in **1** readily promotes far more efficient anion transports than its free monomeric counterpart **G3** by up to 35 folds through a dynamic metal-anion bond (Fig. 1d).

Commercially available **G1**-**G5** were selected to investigate their binding properties with host **1**. ^{1}H NMR experiments were first carried out to evaluate the host-guest complexation in $CDCl_3$. As shown in Figs. 2a-c, mixing **1** and **G3** at 1:2 molar ratio generated one set of proton signals distinctively different from those of free host and free guest, suggesting not only the formation of a new complex but also the association and dissociation between **1** and **G3** to be a fast-exchange process. Specifically, the H_1 signal in **1** shifts up field largely by 0.46 ppm, which indicated that **1** experienced a shielded magnetic environment provided by **G3**. Together with upfield changes in the chemical shift for protons H_2 and H_3 and those from 3.5–4.0 ppm (Fig. S1 in Supporting information) in **1**, we can conclude that the bound **G3** molecules largely reside in the cavity of **1**, likely forming a sandwich supramolecular structure **1**·(**G3**)$_2$. Similarly, **1** is also found to be capable of binding guest molecules of **G1**, **G2**, **G4** and **G5** at 1:2 molar ratio, possibly producing complexes **1**·(**Gn**)$_2$ (Figs. S2-S5 in Supporting information). Additionally, UV-vis and fluorescence experiments were also con-

Table 1
Association constants (K_a) and cooperativity factors (α) for 1:2 complexes formed between **1** and **Gn**s in $CDCl_3$ at 298 K.

Guest	K_{a1} (L/mol)	K_{a2} (L/mol)	Cooperativity factor α ($4K_{a2}/K_{a1}$)
G1	$(4.06 \pm 0.03) \times 10^4$	$(0.40 \pm 0.02) \times 10^2$	0.004
G2	$(1.12 \pm 0.01) \times 10^4$	$(0.56 \pm 0.02) \times 10^2$	0.02
G3	$(4.78 \pm 0.15) \times 10^2$	$(1.63 \pm 0.23) \times 10^2$	1.37
G4	$(1.60 \pm 0.01) \times 10^5$	$(2.63 \pm 0.05) \times 10^2$	0.007
G5	$(4.78 \pm 0.09) \times 10^4$	$(2.86 \pm 0.12) \times 10^2$	0.024

ducted to investigate the complexation process between **1** and **Gn**. As shown in Fig. S34 and S35 (Supporting information), the ultraviolet absorption and fluorescence emission intensity of **Gn** changed dramatically after the addition of 0.5 equiv. of **1**, which further confirmed the formation of complexes **1**·(**Gn**)$_2$.

To quantitatively measure the association constants (K_a) between **1** and **Gn**s (n = 1-5), ^{1}H NMR titrations were conducted by monitoring changes in chemical shift of H_1 in **1**. The mole-ratio plot confirms all binding stoichiometries between **1** and **Gn**s to be 1:2 (Figs. S6-S25 in Supporting information). Accordingly, K_a values were calculated for the 1:2 complexes **1**·(**Gn**)$_2$ using the BindFit software. As summarized in Table 1, while we are not exactly sure why **G3** demonstrates a considerable allosteric binding cooperativity value of 1.37 with $K_{a1} = (4.78 \pm 0.15) \times 10^2$ L/mol and $K_{a2} = (1.63 \pm 0.23) \times 10^2$ L/mol, other non-**G3** guests however show negligible cooperativity, with the first **Gn** bound more tightly than the second **Gn** by 23-334 folds. Moreover, UV-vis spectroscopy Job plot experiments were also performed to determine the stoichiometry of the complex, and the results indicate the formation of a 1:2 complex between **1** and **Gn** (Fig. S32 in Supporting information), which are consistent with those obtained from NMR molar ratio analysis.

Prompted by the high likelihood that the formed sandwich structures **1**·(**Gn**)$_2$ might facilitate cross-membrane anion transport *via* dynamic metal-ligand interaction, we conducted the pH-sensitive HPTS assay, having the intravesicular region filled with 0.1 mmol/L HPTS and 67 mmol/L Na_2SO_4 at pH 7.0 and the extravesicular region with 65 mmol/L Na_2SO_4 and 2.5 mmol/L NaX ($X^- = Cl^-$, Br^-, I^-, NO_3^- and ClO_4^-) at pH 6.0. If **1**·(**Gn**)$_2$ does not transport or transports cations not as well as the anions, the transporter-mediated influx of anions will have to be accompanied by the influx of H^+ or efflux of OH^-, resulting in an increase in intravesicular pH and the fluorescence intensity of the HPTS dye (Fig. 3a). Using this assay and as illustrated in Fig. 3b, among all the tested complexes **1**·(**Gn**)$_2$ at 2.5 μmol/L, only **1**·(**G3**)$_2$ displays a fractional ion transport activity value (R_{Cl^-}) of 92 %, which is much larger than the combined value of 37 % (20 % from **1** at 2.5 μmol/L and 17 % from **G3** at 5.0 μmol/L). Coincidentally yet intriguingly,

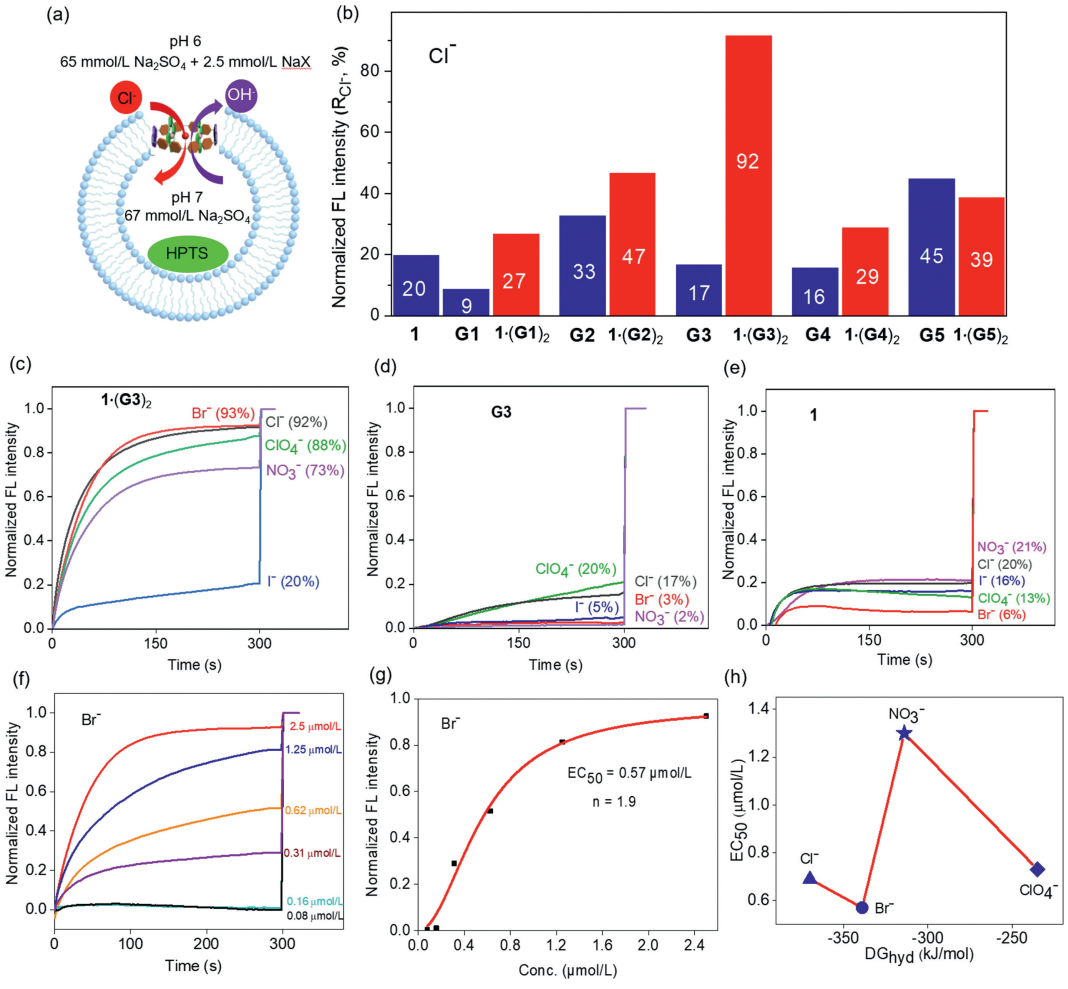


Fig. 3. (a) Schematic illustration of the HPTS assay for measuring the Cl^- transport activity, applying the pH-sensitive HPTS dye trapped inside LUV under a pH gradient of 7 to 6. (b) Anion transport activities (R_{Cl^-}) of **1**, **Gn** and **1**·(**Gn**)$_2$; $R_{Cl^-} = (I_{Cl^-} - I_0)/(I_{Triton} - I_0)$. (c–e) Present anion transport activities for Cl^-, Br^-, I^-, NO_3^- and ClO_4^- by **1**·(**G3**)$_2$, **G3** and **1**. (f) and (g) Illustrate EC_{50} value determination for Br^- for **1**·(**G3**)$_2$. (h) EC_{50} values *vs.* hydration energies for **1**·(**G3**)$_2$-mediated anion transport. HPTS = 8-hydroxypyrene-1,3,6-trisulfonic acid; [**1**] = [**1**·(**G3**)$_2$] = 2.5 μmol/L and [**Gn**] = 5.0 μmol/L.

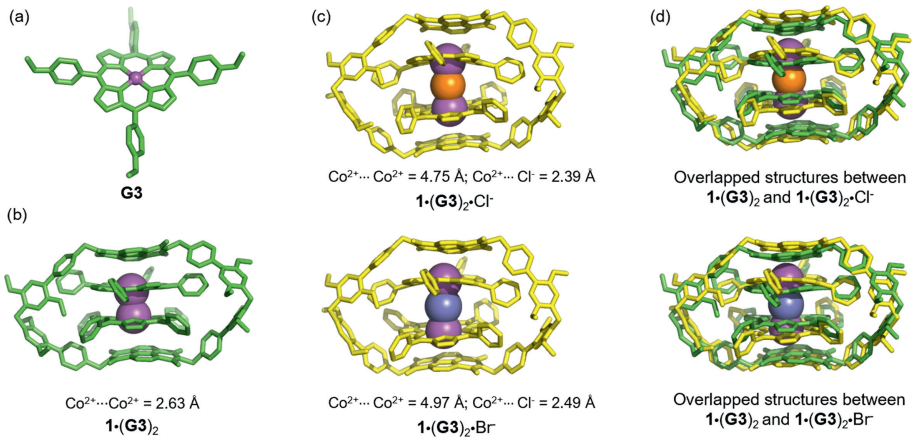


Fig. 4. (a) Crystal structure of **G3**. (b-d) Describe the computationally optimized structures of **1**·(**G3**)$_2$, **1**·(**G3**)$_2$·Cl^- and **1**·(**G3**)$_2$·Br^- at the level of M06-2X/6-31G(d) in the gas phase as well as their overlapped structures.

1·(**G3**)$_2$ is the only complex whereas **1** exhibits a positive cooperativity in binding two molecules of **G3** (Table 1). After considering the transport activities of **1** and **G3** as conservatively estimated in Table S1 (Supporting information), the chloride transport activity of **1**·(**G3**)$_2$ at 2.5 μmol/L is at least 92 %, which is 5.4 times that of **G3** at 5.0 μmol/L.

Applying the same HPTS assay in Fig. 3a after replacing 65 mmol/L Na_2SO_4 + 2.5 mmol/L NaX with 67 mmol/L Na_2SO_4 at pH 8.0, we found that **1**·(**G3**)$_2$ at 2.5 μmol/L elicits no detectable ion transport activity (Fig. S27 in Supporting information). Substituting Na_2SO_4 with K_2SO_4 in both intra- and extravesicular regions leads to the same observation. These findings confirm the inability of **1**·(**G3**)$_2$ to transport both Na^+ and K^+ ions.

Furthermore, enhanced ion transport activities arising from the confined dimeric **G3** are also seen when anions such as Br^-, NO_3^- and ClO_4^- are examined (Figs. 3c-e). Backed by the same method for conservatively estimating transport activity (Table S2 in Supporting information), the anion-transporting capacity of **1**·(**G3**)$_2$ increases by 30 folds for Br^-, 35 folds for NO_3^- and 3.4 folds for ClO_4^- with respect to those of **G3** (Fig. 3c *vs.* 3d).

Using the well-established Hill analysis, the EC_{50} value at which 50 % ion transport activity is reached was determined to be 0.69, 0.57, 1.30 and 0.74 μmol/L for Cl^-, Br^-, NO_3^- and ClO_4^-, respectively (Figs. 3f-h and Fig. S28 in Supporting information).

To evaluate whether the introduction of **1**·(**G3**)$_2$ maintains membrane integrity, we conducted membrane leakage assays. As shown in Fig. S33 (Supporting information), it was found that membrane-lytic melittin results in efflux of 58 % and 99 % CF dye from LUVs at 5 and 25 nmol/L, respectively, but incorporation of **1**·(**G3**)$_2$ at a concentration as high as 2.5 μmol/L produces an only negligible CF efflux of 3 %. These comparative studies clearly support well-maintained membrane integrity in the presence of **1**·(**G3**)$_2$ at high concentrations.

Consistent with the above anion transport studies, ^{1}H NMR titrations verify the ability of **1**·(**G3**)$_2$ to bind various anions. Specifically, addition of 10 equiv. Br^- ion to the solution of **1**·(**G3**)$_2$ in $CDCl_3$ results in significant downfield changes in the chemical shift of H_a and H_1, suggesting the effective binding of Br^- anion by **1**·(**G3**)$_2$. The fact that Br^- exerts considerable impact on H_a from **G3** (Fig. 2b *vs.* 2f) but no influence on H_1 from **1** (Fig. 2c *vs.* 2g) confirms **G3** from **1**·(**G3**)$_2$ to be responsible for the **1**·(**G3**)$_2$-mediated binding of Br^- anions. The additional fact that Br^- makes no difference in chemical shift but does make the shape and height different for both H_a and H_b from **G3** and **1**·(**G3**)$_2$ (Fig. 2e *vs.* 2f) suggests Br^- to interact mainly with **G3** from **1**·(**G3**)$_2$. Further investigations show that **1**·(**G3**)$_2$ can also bind Cl^-, NO_3^- and ClO_4^- (Figs. S29-S31 in Supporting information).

To elucidate the structural basis for the anion transport activity of complex **1**·(**G3**)$_2$, we sought to characterize its solid-state structure. Despite repeated attempts, we were unable to obtain single crystals of the complex. Instead, crystallization invariably resulted in the separation of pure host **1** or guest **G3** (CCDC No. 2492337, Fig. 4a). With a stoichiometry 1:2 molar ratio inferred from the solution binding profile, we applied M06-2X/6-31G(d) to optimize complexes of **1**·(**G3**)$_2$ with and without Cl^- or Br^- (Figs. 4b-d). The computed structures reveal the formation of a Co^{2+}···Co^{2+} bond of 2.63 Å inside the macrocycle-confirmed dimeric metalloporphyrin (Fig. 4b). This results in a tightly packed complex **1**·(**G3**)$_2$, seemingly leaving no entrance space for anions. Nevertheless, the presence of Cl^- and Br^- appears to break the Co^{2+}···Co^{2+} bond, increasing the Co^{2+}···Co^{2+} distances to 4.75 Å and 4.97 Å (Fig. 4c), respectively. Together with the overlapped structures shown in Fig. 4d, these computational findings suggest a highly dynamic nature of the cage structure and its associated complexes as well as dynamic metal-anion interactions, enabling the dynamic formation of the Co^{2+}···Co^{2+} and Co^{2+}-anion bonds and their subsequent breaking for the anion to bind and release when crossing the membrane as sketched in Fig. 1d.

To summarize, we have successfully demonstrated a previously unexplored strategy toward construction of an artificial anion-transporting system. This was achieved by using a giant macrocycle to bind and constrain two Co^{2+}-porphyrin complexes in its large adaptive tubular cavity while leaving sufficiently large, confined space for anions to bind and release through dynamic metal-anion interactions. This strategy effectively converts an uncompetitive transporter Co^{2+}-porphyrin into a highly efficient anion-transporting, sandwiched host-guest complex, displaying good EC_{50} values of 0.57–1.30 μmol/L for Cl^-, Br^-, ClO_4^- and NO_3^- and activity enhancements by up to 35 folds over monomeric Co^{2+}-porphyrin. This geometric confinement-based approach might instigate others or find new inspiring uses in designing diverse types of artificial transmembrane transporter systems, possibly benefiting multidisciplinary applications in chemistry, materials sciences, biology and medicines.

Declaration of competing interest

The authors declare that they have no known competing financialinterestsor personal relationships that could have appeared to influence the work reported in this paper.

CRediT authorship contribution statement

Fei Zeng: Writing – original draft, Investigation. **Xinrui Pan:** Investigation. **Zihong Yang:** Investigation, Data curation. **Jie Shen:** Writing – review & editing. **Wenju Chang:** Writing – review & editing. **Huaqiang Zeng:** Writing – review & editing, Supervision.

Acknowledgments

This work was supported by the National Natural Science Foundation of China (Nos. 22501049, 21602055, 22271049 and 22371048), Natural Science Foundation of Hunan Province (No. 2023JJ50414), Natural Science Foundation of Fujian Province (No. 2025J08021) and a start-up grant from Fuzhou University.

Supplementary materials

Supplementary material associated with this article can be found, in the online version, at doi:10.1016/j.cclet.2025.112355.

References

[1] T.J. Jentsch, Curr. Opin. Neurobiol. 6 (1996) 303–310.
[2] K.S. Suh, S.H. Yuspa, Curr. Pharm. Des. 11 (2005) 2753–2764.
[3] J.L. Sessler, L.R. Eller, W.S. Cho, et al., Angew. Chem. Int. Ed. 44 (2005) 5989–5992.
[4] A.P. Davis, D.N. Sheppard, B.D. Smith, Chem. Soc. Rev. 36 (2007) 348–357.
[5] J.T. Davis, O. Okunola, R. Quesada, Chem. Soc. Rev. 39 (2010) 3843–3862.
[6] S.K. Ko, S.K. Kim, A. Share, et al., Nat. Chem. 6 (2014) 885–892.
[7] V. Soto-Cerrato, P. Manuel-Manresa, E. Hernando, et al., J. Am. Chem. Soc. 137 (2015) 15892–15898.
[8] T. Saha, M.S. Hossain, D. Saha, et al., J. Am. Chem. Soc. 138 (2016) 7558–7567.
[9] X.Q. Hong, Y.Y. Xing, Z.K. Wang, et al., Chin. Chem. Lett. 32 (2021) 1653–1656.
[10] S.H. Park, S.H. Park, E.N.W. Howe, et al., Chem 5 (2019) 2079–2098.
[11] B. Bishop, S. Huang, H. Chen, et al., Chin. Chem. Lett. 35 (2024) 109966.
[12] X. Wu, A.M. Gilchrist, P.A. Gale, Chem 6 (2020) 1296–1309.
[13] J.T. Davis, P.A. Gale, R. Quesada, Chem. Soc. Rev. 49 (2020) 6056–6086.
[14] X. Hu, B. Song, S. Song, et al., Chin. Chem. Lett. 36 (2025) 110918.
[15] J. de Jong, J.E. Bos, S.J. Wezenberg, et al., Chem. Rev. 123 (2023) 8530–8574.
[16] R. Cao, R.B. Rossdeutcher, Y. Zhong, et al., Nat. Chem. 15 (2023) 1559–1568.
[17] X. Wei, G. Zhang, Y. Shen, et al., J. Am. Chem. Soc. 138 (2016) 2749–2754.
[18] S.P. Zheng, L.B. Huang, Z. Sun, et al., Angew. Chem. Int. Ed. 60 (2021) 566–597.
[19] X. Jiang, L. Wang, S. Liu, et al., Mater. Chem. Front. 5 (2021) 1610–1631.
[20] J. Yang, G. Yu, J.L. Sessler, et al., Chem 7 (2021) 3256–3291.
[21] M. Merritt, M. Lanier, G. Deng, et al., J. Am. Chem. Soc. 120 (1998) 8494–8501.
[22] P.H. Schlesinger, R. Ferdani, J. Liu, et al., J. Am. Chem. Soc. 124 (2002) 1848–1849.
[23] V. Sidorov, F.W. Kotch, G. Abdrakhmanova, et al., J. Am. Chem. Soc. 124 (2002) 2267–2278.
[24] P.V. Santacroce, J.T. Davis, M.E. Light, et al., J. Am. Chem. Soc. 129 (2007) 1886–1887.
[25] X. Li, B. Shen, X.Q. Yao, et al., J. Am. Chem. Soc. 129 (2007) 7264–7265.
[26] J.T. Davis, P.A. Gale, O.A. Okunola, et al., Nat. Chem. 1 (2009) 138–144.
[27] C.R. Yamnitz, S. Negin, I.A. Carasel, et al., Chem. Commun. 46 (2010) 2838–2840.
[28] H. Valkenier, L.W. Judd, H. Li, et al., J. Am. Chem. Soc. 136 (2014) 12507–12512.
[29] Y.R. Choi, B. Lee, J. Park, et al., J. Am. Chem. Soc. 138 (2016) 15319–15322.
[30] A. Kerckhoffs, M.J. Langton, Chem. Sci. 11 (2020) 6325–6331.
[31] H. Chen, Y. Liu, X. Cheng, et al., Angew. Chem. Int. Ed. 60 (2021) 10833–10841.
[32] Z. Zhao, M. Zhang, B. Tang, et al., Front. Chem. 8 (2021) 621323.
[33] D. Mondal, M. Ahmad, B. Dey, et al., Nat. Commun. 13 (2022) 6507.
[34] T.G. Johnson, A. Sadeghi-Kelishadi, M.J. Langton, J. Am. Chem. Soc. 144 (2022) 10455–10461.
[35] S.J. Wezenberg, L.J. Chen, J.E. Bos, et al., J. Am. Chem. Soc. 144 (2022) 331–338.
[36] X. Wu, P. Wang, W. Lewis, et al., Nat. Commun. 13 (2022) 4623.
[37] M. Ahmad, N.J. Roy, A. Singh, et al., Chem. Sci. 14 (2023) 8897–8904.
[38] A.V. Jentzsch, D. Emery, J. Mareda, et al., Nat. Commun. 3 (2012) 905.
[39] A. Vargas Jentzsch, S. Matile, J. Am. Chem. Soc. 135 (2013) 5302–5303.
[40] C. Ren, X. Ding, A. Roy, Chem. Sci. 9 (2018) 4044–4051.
[41] T.G. Johnson, A. Docker, A. Sadeghi-Kelishadi, et al., Chem. Sci. 14 (2023) 5006–5013.
[42] S. Benz, M. Macchione, Q. Verolet, et al., J. Am. Chem. Soc. 138 (2016) 9093–9096.
[43] L. Yuan, P. Jiang, J. Hu, et al., Chin. Chem. Lett. 33 (2022) 2026–2030.
[44] A. Docker, T.G. Johnson, H. Kuhn, et al., J. Am. Chem. Soc. 145 (2023) 2661–2668.
[45] L.M. Lee, M. Tsemperouli, A.I. Poblador-Bahamonde, et al., J. Am. Chem. Soc. 141 (2019) 810–814.
[46] G. Park, D.J. Brock, J.P. Pellois, et al., Chem 5 (2019) 2215–2227.
[47] V. Gorteau, G. Bollot, J. Mareda, et al., J. Am. Chem. Soc. 128 (2006) 14788–14789.
[48] W.L. Huang, X.D. Wang, Y.F. Ao, et al., J. Am. Chem. Soc. 142 (2020) 13273–13277.
[49] W.L. Huang, X.D. Wang, Y.F. Ao, et al., Angew. Chem. Int. Ed. 62 (2023) e202302198.
[50] C. Zhang, J. Tian, S. Qi, et al., Nano Lett. 20 (2020) 3627–3632.
[51] G. Park, F.P. Gabbaï, Angew. Chem. Int. Ed. 59 (2020) 5298–5302.
[52] B.P. Benke, P. Aich, Y. Kim, J. Am. Chem. Soc. 139 (2017) 7432–7435.
[53] C.J.E. Haynes, J. Zhu, C. Chimerel, et al., Angew. Chem. Int. Ed. 56 (2017) 15388–15392.
[54] C.L. Ren, F. Zeng, J. Shen, et al., J. Am. Chem. Soc. 140 (2018) 8817–8826.
[55] F. Zeng, F. Liu, L. Yuan, et al., Org. Lett. 21 (2019) 4826–4830.
[56] L. Yuan, J. Shen, R.J. Ye, et al., Chem. Commun. 55 (2019) 4797–4800.
[57] A. Roy, H. Joshi, R.J. Ye, et al., Angew. Chem. Int. Ed. 59 (2020) 4806–4813.
[58] M. El-Etri, J. Cuppoletti, Am. J. Physiol. 270 (1996) L386–L392.
[59] F.X. Wang, J.W. Liu, X.Q. Hong, et al., CCS Chem. 4 (2022) 2409–2419.
[60] F. Zeng, L.L. Tang, M.H. Ding, et al., Org. Lett. 25 (2023) 6290–6294.
[61] X.N. Han, Q.S. Zong, Y. Han, et al., CCS Chem. 4 (2022) 318–330.